

Lamb Shift and Sub-Compton Electron Dynamics: Dirac Hydrogen Wavefunctions without Singularities

Lloyd Watts

October 31, 2016

| | |
|--|-----------|
| 1. INTRODUCTION..... | 3 |
| 2. POSSIBLE CHARGE DISTRIBUTIONS..... | 3 |
| 2.1. CHARGED SHELL DISTRIBUTION INSPIRED BY HESTENES' SPACE-TIME ALGEBRA..... | 4 |
| 2.2. IMAGINARY CHARGED RING INSPIRED BY BARUT AND BRACKEN'S ZITTERBEWEGUNG ANALYSIS | 4 |
| 2.3. GAUSSIAN CHARGE DENSITY | 5 |
| 2.4. EXPONENTIAL CHARGE DENSITY | 5 |
| 3. ANALYTIC SOLUTIONS FOR SCHRODINGER AND DIRAC WAVEFUNCTIONS | 8 |
| 4. NUMERICAL SOLUTION FOR MODIFIED DIRAC WAVEFUNCTION | 12 |
| 4.1. ENERGY AND ELECTRON WAVEFUNCTION FOR THE $1S^{1/2}$ STATE | 13 |
| 5. IMPLICATIONS FOR A FREE ELECTRON..... | 19 |
| 6. FREE ELECTRON NUMERICAL SIMULATIONS – PRIOR 1D, 2D | 21 |
| 6.1. 1D | 22 |
| 6.2. 2D | 23 |
| 7. FREE ELECTRON NUMERICAL SIMULATIONS – NEW 1D, 2D, 3D | 24 |
| 7.1. 1D SUPER-NARROW | 25 |
| 7.2. 2D SUPER-NARROW | 26 |
| 7.3. 3D TIGHT GAUSSIAN | 28 |
| 7.4. 3D VERY TIGHT GAUSSIAN | 29 |
| 7.5. 3D SPHERICAL SHELL | 30 |
| 8. MODIFYING THE DIRAC EQUATION TO GET A STABLE CONFIGURATION..... | 30 |
| 9. DISCUSSION | 31 |
| 10. CONCLUSIONS..... | 33 |
| REFERENCES | 34 |
| APPENDIX – PERTURBATION ANALYSIS FOR GAUSSIAN CHARGE DENSITY | 35 |

Abstract – The Schrodinger Hydrogen Atom does not explain spin or fine structure, and has wavefunctions with cusps at the origin. The Dirac Hydrogen Atom explains spin and fine structure, but does not explain Lamb Shift, and has wavefunctions that are singular at the origin. Quantum Electrodynamics (QED) explains Lamb Shift but appears to be silent on how the wavefunctions are affected and whether the wavefunction singularities are removed. In this work, we use perturbation analysis to show that the Lamb Shift is consistent with electron charge spreading inside the half-reduced Compton Wavelength, and we develop a novel numerical technique for solving the Dirac Hydrogen problem with a modified Coulomb potential, and use it to find the form of the modified Dirac Hydrogen wavefunctions. We show that the singularity at the origin of the Dirac Hydrogen wavefunction is eliminated, with a small amount of charge density near the origin displaced radially outward. The large component is made continuous at the origin, and the small component is driven to zero at the origin. The near-constant behavior of the Bethe Logarithm out to its asymptotic limit as principal quantum number $n \rightarrow \infty$ leads to a novel suggestion that this charge spreading for a bound electron in a Hydrogen Atom may also occur for a free electron. We also show novel 3D visualizations of numerical Dirac equation simulations.

1. Introduction

Our modern understanding of the electron is based on the Dirac Equation (Dirac, 1928), which predicts Hydrogen energy levels up to the level of fine structure, and Quantum Electrodynamics (QED) (Feynman, 1948), which provides additional small energy level corrections to account for the Lamb Shift (Lamb and Retherford, 1948) and other important refinements. In QED, the Lamb Shift is understood as based on electron self-interaction, in which the electron “continuously emits and absorbs virtual photons, and as a result its electric charge is spread over a finite volume instead of being pointlike.” [Eides, Groth, and Shelyuto, 2007] But QED is focused on computing the energy levels in a momentum space treatment using perturbation analysis, and appears to be silent on how exactly the charge is spread over that small volume in position space.

Can we interpret this charge spreading as an effective localized charge distribution based on the electron wavefunction? What is the charge distribution in position space, and exactly how large is the volume over which the charge is spread? What is the three-dimensional shape of the distribution? Is there some internal motion to this charge distribution? Does this distribution change size or shape, or move differently, depending on whether the electron is free or bound in an atom, or how tightly it is bound? The wavefunctions for the Dirac Hydrogen atom are known exactly in closed form, but they have singularities at the nucleus (Darwin, 1928). We know that QED provides the necessary Lamb Shift correction, but does it also tame the singularities in the wavefunction at the nucleus of the atom? If so, what is the shape of the corrected wavefunction near the nucleus? With the exception of Welton (1948), who gave an early, informal argument about the mean-square fluctuations in the position of the electron, mainstream QED literature appears to be silent on all of these points.

If we had definitive answers to these questions, we could claim to have an understanding of the behavior of the electron on very small spatial scales, such that its effect is evident in the vicinity of the atomic nucleus, not just an accurate assessment of its energy. And furthermore, we hope that a better understanding of the small-scale behavior of the electron might reveal deeper insights into the physical process of photon absorption and emission in quantum transitions, since we expect that a correct analysis of a quantum transition will require corrected, non-singular Dirac wavefunctions for both the initial and final state of the atom.

The purpose of this paper is to examine what insights may be inferred about this small-scale electron behavior from existing experimental data and QED theory.

2. Possible Charge Distributions

At the present time, there is no definitive accepted theory that would establish the form of the localized electron charge distribution corresponding to the dominant QED self-interaction and vacuum polarization effects. In the absence of such a definitive theory, let us consider various

proposals that have been put forth in the literature; by examining of all of them together, we will see several important common properties which we may expect to hold true for the final, correct theory.

2.1. Charged Shell Distribution inspired by Hestenes' Space-Time Algebra

David Hestenes (2010) uses his Space-Time Algebra to reformulate the solution to the Dirac Equation in the canonical form $\psi = (\rho e^{i\beta})^{\frac{1}{2}} R$, which includes a statistical charge distribution ρ . Later, he describes a free electron as a point charge moving on a helical path with a "zitter" radius of $r_z = \frac{\lambda_c}{2}$, where $\lambda_c = \frac{h}{mc}$ is the Reduced Compton Wavelength for the electron.

We begin by exploring the hypothesis, following Hestenes, that an electron is in a very fast circular or helical motion about its center of mass with radius r_z . In a Hydrogen atom, assuming a spin- $\frac{1}{2}$ precessing motion, we hypothesize that the net result is that, from the frame of reference of the nucleus of a Hydrogen atom, the charge appears to be distributed in very fast motion on a small sphere of radius r_z – we will call this the **Charged Shell** charge distribution. This leads to a charge probability distribution of $\rho(r) = \frac{q}{4\pi r_z^2} \delta(r - r_z)$, which leads to a modified Coulomb potential of

$$V_{mod}(r) = -\frac{q^2}{4\pi\epsilon_0 \text{Max}(r, r_z)}$$

which was first analyzed by Wannier (Cutoff Coulomb Potential, 1943). After a first-order perturbation analysis, this modified potential leads to agreement with existing QED theory on the leading term of the Lamb Shift when

$$r_z \approx \frac{\lambda_c}{2} (0.38126)$$

We note that this radius is smaller than Hestenes' proposed zitter radius by a factor of about $\frac{1}{2.623}$.

2.2. Imaginary Charged Ring inspired by Barut and Bracken's Zitterbewegung Analysis

Similarly, Barut and Bracken [1981] re-examined Zitterbewegung and offered an interpretation of the electron as a "massless charge performing a complicated motion around a center of mass". In their model, the charge moves in a circle of radius r_z in two hidden spatial dimensions. This leads to a charge probability distribution of

$$\rho(r) = \frac{q}{4\pi r_z^2} \delta(r - ir_z),$$

which leads to a modified Coulomb potential of

$$V_{mod}(r) = -\frac{q^2}{4\pi\epsilon_0 \sqrt{r^2 + r_z^2}}$$

which was first analyzed by Patil (Second-Order Truncated Coulomb Potential, 1981). After a first-order perturbation analysis, this modified potential leads to agreement with existing QED theory on the leading term of the Lamb Shift when

$$r_z \approx \frac{\lambda_c}{2} * (0.082364)$$

We note that this radius is smaller than Hestenes' proposed zitter radius by a factor of about $\frac{1}{12.14}$.

2.3. Gaussian Charge Density

In this model, the charge would have a 3D Gaussian distribution because it is being buffeted by virtual photons in a kind of Brownian Motion. Recent work by Bracken [2006, 2012] has made a connection between the Dirac Equation and Quantum Random Walks, which may appear to support the idea of a Gaussian charge distribution. This leads to a charge probability distribution of

$$\rho(r) = \frac{1}{2\sqrt{2}\pi^{3/2}r_z^3} e^{-\frac{r^2}{2r_z^2}},$$

which leads to a modified Coulomb potential of

$$V_{mod}(r) = -\frac{q^2}{4\pi\epsilon_0 r} \text{Erf}\left(\frac{r}{\sqrt{2} r_z}\right).$$

After a first-order perturbation analysis, this modified potential leads to agreement with existing QED theory on the leading term of the Lamb Shift when

$$r_z \approx \frac{\lambda_c}{2} (0.21885)$$

Details of the perturbation analysis for the Gaussian Charge Density are given in the Appendix.

2.4. Exponential Charge Density

In this model, the charge would have an exponential distribution, as though in the Spherical Harmonic ground state of an attracting charge, possibly represented by the "small component" of the Dirac Equation solution, which represents a negative energy solution and could possibly be seen as representing a virtual positron associated with the electron. This leads to a charge probability distribution of

$$\rho(r) = \frac{q}{\pi r_z^3} e^{-\frac{2r}{r_z}},$$

which leads to a modified Coulomb potential of

$$V_{mod}(r) = -\frac{q^2}{4\pi\epsilon_0 r} \left(1 - e^{-\frac{2r}{r_z}} \left(1 + \frac{r}{r_z}\right)\right)$$

After a first-order perturbation analysis, this modified potential leads to agreement with existing QED theory on the leading term of the Lamb Shift when

$$r_z \approx \frac{\lambda_c}{2} (0.21885)$$

In Table 1, we give a summary of the Charge Distributions, Modified Coulomb Potentials, and Characteristic Radius which corresponds to the leading term of the Lamb Shift. In Figure 1, we plot the Modified Coulomb Potentials corresponding to the leading term of the Lamb Shift.

| Charge Distribution Type | Charge Distribution and Modified Coulomb Potential | Characteristic Radius to match Lamb Shift |
|----------------------------------|--|--|
| Point Charge | $\rho(r) = q\delta(r)$ $V(r) = -\frac{q^2}{4\pi\epsilon_0 r}$ | n/a |
| Charged Shell | $\rho(r) = \frac{q}{4\pi r_z^2} \delta(r - r_z)$ $V_{mod}(r) = -\frac{q^2}{4\pi\epsilon_0 \text{Max}(r, r_z)}$ | $r_z \approx \frac{\lambda_c}{2} (0.38126)$ |
| Zitterbewegung Imaginary Ring | $\rho(r) = \frac{q}{4\pi r_z^2} \delta(r - ir_z)$ $V_{mod}(r) = -\frac{q^2}{4\pi\epsilon_0 \sqrt{r^2 + r_z^2}}$ | $r_z \approx \frac{\lambda_c}{2} (0.082364)$ |
| Gaussian Charge Density | $\rho(r) = \frac{q}{2\sqrt{2}\pi^{3/2} r_z^3} e^{-\frac{r^2}{2r_z^2}}$ $V_{mod}(r) = -\frac{q^2}{4\pi\epsilon_0 r} \text{Erf}\left(\frac{r}{\sqrt{2} r_z}\right)$ | $r_z \approx \frac{\lambda_c}{2} (0.21885)$ |
| Exponential Charge Density | $\rho(r) = \frac{q}{\pi r_z^3} e^{-\frac{2r}{r_z}}$ $V_{mod}(r) = -\frac{q^2}{4\pi\epsilon_0 r} \left(1 - e^{-\frac{2r}{r_z}} \left(1 + \frac{r}{r_z}\right)\right)$ | $r_z \approx \frac{\lambda_c}{2} (0.21885)$ |

Table 1. Charge Distributions, Modified Coulomb Potentials, and Characteristic Radii. Except for the Point Charge distribution, all of these proposals are consistent with the leading term of the Lamb Shift.

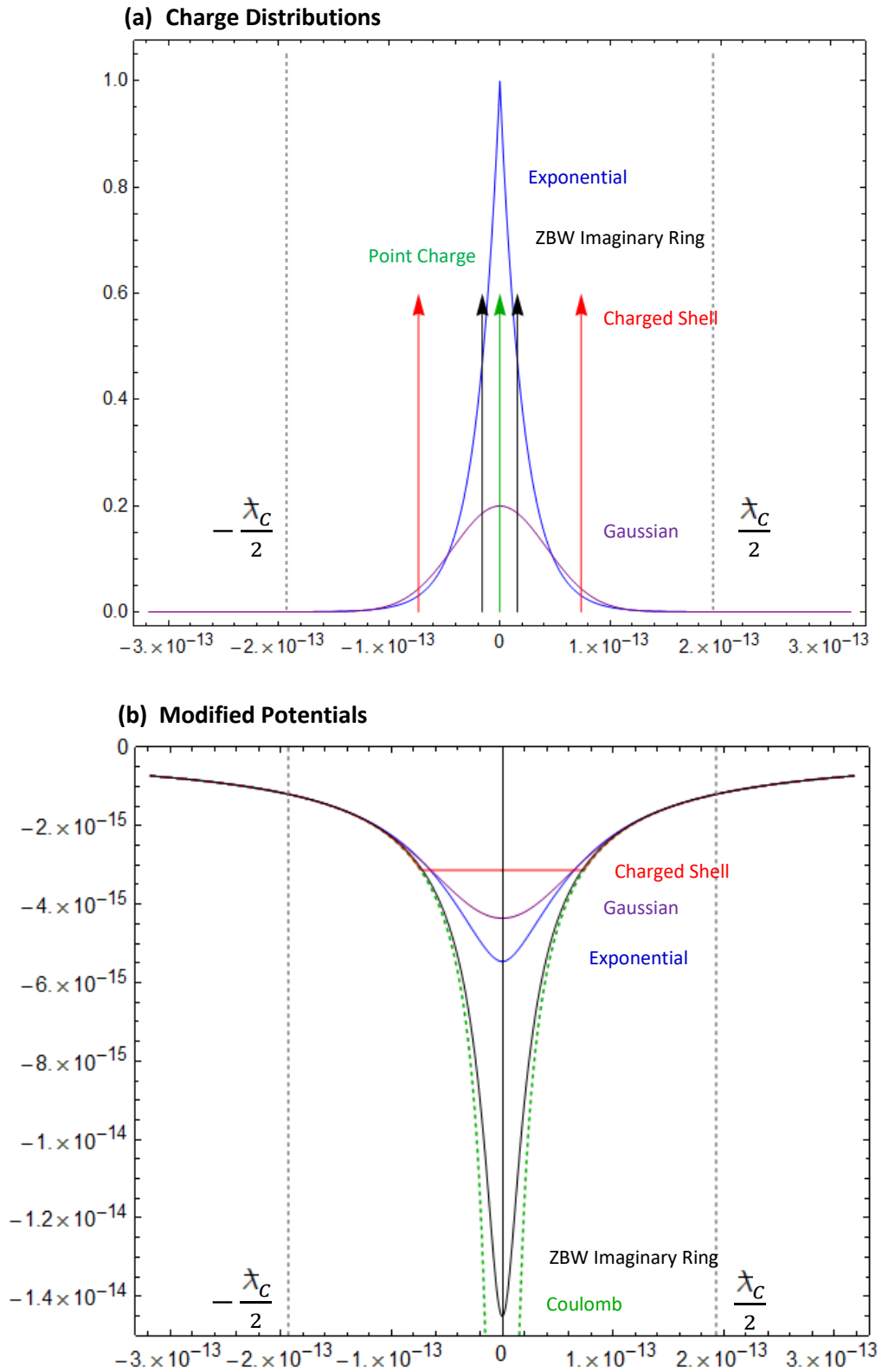


Figure 1. (a) Charge Distributions, and (b) Modified Coulomb Potentials, consistent with the leading term of the Lamb Shift.

For all of the proposals, the Lamb Shift implies that the electron's charge distribution in a bound state must be contained well inside a sphere whose radius is half the Reduced Compton Wavelength.

So far, we can say that Lamb Shift implies tight localization of any of the charge density proposals for the bound state case, well within a radius of half the Reduced Compton Wavelength. For this reason, we will use the term "Sub-Compton Electron Charge Density".

3. Analytic Solutions for Schrodinger and Dirac Wavefunctions

The usual non-relativistic time-independent Schrödinger equation for the Hydrogen atom is

$$\frac{\hbar^2}{2m} \nabla^2 \psi(r, \theta, \phi) + (E - V(r)) \psi(r, \theta, \phi) = 0 ,$$

where $\psi(r, \theta, \phi)$ is the single-component wavefunction in spherical coordinates, E is the energy, m is the mass of the electron, and $V(r)$ is the central potential due to the positively charged nucleus. The usual assumption is that the nucleus is a non-moving point charge, which implies an infinitely heavy nucleus with infinitely high charge density in zero volume, leading to the central Coulomb potential

$$V(r) = -\frac{q^2}{4\pi\epsilon_0 r} = -\frac{\hbar^2}{ma_0 r} ,$$

which is obviously singular at the origin. The wavefunction solutions for the non-relativistic Schrodinger equation are well-known, and shown for the first few quantum states in Table 2:

| State | Normalized Radial Solution | Normalized Wavefunction Solution |
|-------|--|--|
| 1S | $R_{1S}(r) = \frac{2}{a_0^{3/2}} e^{-\frac{r}{a_0}}$ | $\psi_{1S}(r) = \frac{1}{\sqrt{\pi} a_0^{3/2}} e^{-\frac{r}{a_0}}$ |
| 2S | $R_{2S}(r) = \frac{1}{2\sqrt{2} a_0^{3/2}} \left(2 - \frac{r}{a_0}\right) e^{-\frac{r}{2a_0}}$ | $\psi_{2S}(r) = \frac{1}{4\sqrt{2\pi} a_0^{3/2}} \left(2 - \frac{r}{a_0}\right) e^{-\frac{r}{2a_0}}$ |
| 2P | $R_{2P}(r) = \frac{1}{2\sqrt{6} a_0^{3/2}} \frac{r}{a_0} e^{-\frac{r}{2a_0}}$ | $\psi_{2P}(r) = \frac{1}{4\sqrt{2\pi} a_0^{3/2}} \frac{r \cos \theta}{a_0} e^{-\frac{r}{2a_0}}$ |

Table 2. First few solutions for Schrodinger Hydrogen Atom.

The usual relativistic time-independent Dirac equation for the Hydrogen atom is

$$(-c(\alpha_x p_x + \alpha_y p_y + \alpha_z p_x) - \beta mc^2) \Psi + (E - V(r)) \Psi = 0$$

where Ψ is the four-component (bi-spinor) wavefunction, the non-commuting matrices are defined conventionally as

$$\alpha_x = \begin{bmatrix} 0 & 0 & 0 & 1 \\ 0 & 0 & 1 & 0 \\ 0 & 1 & 0 & 0 \\ 1 & 0 & 0 & 0 \end{bmatrix}, \quad \alpha_y = \begin{bmatrix} 0 & 0 & 0 & -i \\ 0 & 0 & i & 0 \\ 0 & -i & 0 & 0 \\ i & 0 & 0 & 0 \end{bmatrix}, \quad \alpha_z = \begin{bmatrix} 0 & 0 & 1 & 0 \\ 0 & 0 & 0 & -1 \\ 1 & 0 & 0 & 0 \\ 0 & -1 & 0 & 0 \end{bmatrix}, \quad \beta = \begin{bmatrix} 1 & 0 & 0 & 0 \\ 0 & 1 & 0 & 0 \\ 0 & 0 & -1 & 0 \\ 0 & 0 & 0 & -1 \end{bmatrix},$$

Following Landau and Lifshitz, after separation of variables

$$\Psi(r, \theta, \phi) = \begin{pmatrix} \phi(r, \theta, \phi) \\ \chi(r, \theta, \phi) \end{pmatrix} = \begin{pmatrix} f(r)\Omega_{jlm}(\theta, \phi) \\ (-1)^{\frac{1}{2}(1+l-l')} g(r)\Omega_{jl'm}(\theta, \phi) \end{pmatrix},$$

where $l = j \pm \frac{1}{2}$ and $l' = 2j - l$. The radial part of the equation is

$$\begin{aligned} f'(r) + \frac{1+\kappa}{r} f(r) - \frac{1}{\hbar c} (E + mc^2 - V(r))g(r) &= 0 \\ g'(r) + \frac{1-\kappa}{r} g(r) + \frac{1}{\hbar c} (E - mc^2 - V(r))f(r) &= 0 \end{aligned}$$

where

$$\begin{aligned} \kappa &= -\left(j + \frac{1}{2}\right) = -(l + 1) \quad \text{for } j = l + \frac{1}{2} \\ &= +\left(j + \frac{1}{2}\right) = l \quad \text{for } j = l - \frac{1}{2}. \end{aligned}$$

The well-known energy solution is

$$E_{nlj} = \frac{mc^2}{\sqrt{1 + \frac{\alpha^2}{\left(n - \left(j + \frac{1}{2}\right) + \sqrt{\left(j + \frac{1}{2}\right)^2 - \alpha^2}\right)^2}}}$$

where the Fine Structure Constant α is defined as

$$\alpha = \frac{q^2}{4\pi\epsilon_0\hbar c} \approx \frac{1}{137.035999074}.$$

Landau and Lifshitz (1982) provide the full general equations for the normalized radial wavefunction solutions:

$$\begin{aligned} f(r) &= \frac{(2\lambda)^{\frac{3}{2}}}{\Gamma(2\lambda + 1)} \sqrt{\frac{(mc^2 + E)\Gamma(2\lambda + n_r + 1)}{4mc^2 \left(\frac{\alpha mc^2}{\lambda}\right) \left(\frac{\alpha mc^2}{\lambda} - \kappa\right) \cdot n_r!}} (2\lambda r)^{\gamma-1} e^{-\lambda r} \\ &\quad \times \left(\left(\frac{\alpha mc^2}{\lambda} - \kappa\right) {}_1F_1(-n_r; 2\lambda + 1; 2\lambda r) - n_r {}_1F_1(1 - n_r; 2\lambda + 1; 2\lambda r) \right) \end{aligned}$$

$$g(r) = -\frac{(2\lambda)^{\frac{3}{2}}}{\Gamma(2\lambda + 1)} \sqrt{\frac{(mc^2 - E)\Gamma(2\lambda + n_r + 1)}{4mc^2 \left(\frac{\alpha mc^2}{\lambda}\right) \left(\frac{\alpha mc^2}{\lambda} - \kappa\right) \cdot n_r!}} (2\lambda r)^{\gamma-1} e^{-\lambda r} \\ \times \left(\left(\frac{\alpha mc^2}{\lambda} - \kappa\right) {}_1F_1(-n_r; 2\lambda + 1; 2\lambda r) + n_r {}_1F_1(1 - n_r; 2\lambda + 1; 2\lambda r) \right)$$

where

$$\lambda = \frac{mc^2 \sqrt{1 - \left(\frac{E}{mc^2}\right)^2}}{\hbar c}$$

$$\gamma = \sqrt{\kappa^2 - \alpha^2}$$

$$n_r = n - |\kappa|$$

and the normalization conditions are

$$\int_0^\infty (f(r)^2 + g(r)^2) r^2 dr = 1 \quad \text{and} \quad \int_0^\infty \int_0^\pi \int_0^{2\pi} |\Psi_{n,l}|^2 r^2 \sin \theta d\phi d\theta dr = 1$$

3.1.1. $1S_{1/2}$ state

In the particular case of the $1S_{1/2}$ ground state where $n = 1$, $l = 0$, and $j = \frac{1}{2}$, we have $l' = 1$, $\kappa = -1$, $n_r = 0$, which leads to

$$E_{1S_{1/2}} = mc^2 \sqrt{1 - \alpha^2}$$

Substituting those into the radial equations leads to the full system of equations and boundary conditions

$$\begin{aligned} f_{1S_{1/2}}'(r) - \left(\frac{1 + \sqrt{1 - \alpha^2}}{\alpha a_0} + \frac{\alpha}{r} \right) g_{1S_{1/2}}(r) &= 0 \\ g_{1S_{1/2}}'(r) + \frac{2}{r} g_{1S_{1/2}}(r) + \left(\frac{-1 + \sqrt{1 - \alpha^2}}{\alpha a_0} + \frac{\alpha}{r} \right) f_{1S_{1/2}}(r) &= 0 \\ f_{1S_{1/2}}(\infty) &= 0 \\ g_{1S_{1/2}}(\infty) &= 0 \\ \int_0^\infty (f_{1S_{1/2}}(r)^2 + g_{1S_{1/2}}(r)^2) r^2 dr &= 1 \end{aligned}$$

The ground state radial solutions are

$$f_{1S^{1/2}}(r) = \frac{2}{a_0^{3/2}} e^{-\frac{r}{a_0}} \left(\frac{2r}{a_0}\right)^{-1+\sqrt{1-\alpha^2}} \sqrt{\frac{1+\sqrt{1-\alpha^2}}{\Gamma(1+2\sqrt{1-\alpha^2})}}$$

$$g_{1S^{1/2}}(r) = -\frac{\alpha}{1+\sqrt{1-\alpha^2}} f_{1S^{1/2}}(r) \approx -\frac{\alpha}{2} f_{1S^{1/2}}(r)$$

Note that

$$\sqrt{\frac{1+\sqrt{1-\alpha^2}}{\Gamma(1+2\sqrt{1-\alpha^2})}} \approx 1.000018$$

Because $|g(r)|$ is smaller than $|f(r)|$ by about a factor of $\frac{\alpha}{2}$, or about $\frac{1}{274.072}$, $f(r)$ is often called the *large component*, and $g(r)$ is often called the *small component*. Note that since

$$R_{1S}(r) = \frac{2}{a_0^{3/2}} e^{-\frac{r}{a_0}}$$

it follows that

$$f_{1S^{1/2}}(r) = R_{1S}(r) \left(\frac{2r}{a_0}\right)^{-1+\sqrt{1-\alpha^2}} \sqrt{\frac{1+\sqrt{1-\alpha^2}}{\Gamma(1+2\sqrt{1-\alpha^2})}}$$

i.e., the Dirac radial solution is related to the Schrodinger radial solution in a fairly straightforward way.

The full wavefunction solution for the relativistic Dirac equation for the ground state, including the angular bi-spinor components, for the electron spin-up and spin-down states, is given by

$$\Psi_{1S^{1/2}down} = \frac{1}{\sqrt{\pi}a_0^{3/2}} e^{-\frac{r}{a_0}} \left(\frac{2r}{a_0}\right)^{-1+\sqrt{1-\alpha^2}} \sqrt{\frac{1+\sqrt{1-\alpha^2}}{\Gamma(1+2\sqrt{1-\alpha^2})}} \begin{pmatrix} 0 \\ 1 \\ \frac{\alpha}{1+\sqrt{1-\alpha^2}} \begin{pmatrix} i e^{-i\phi} \sin \theta \\ -i \cos \theta \end{pmatrix} \end{pmatrix}$$

$$\Psi_{1S^{1/2}up} = \frac{1}{\sqrt{\pi}a_0^{3/2}} e^{-\frac{r}{a_0}} \left(\frac{2r}{a_0}\right)^{-1+\sqrt{1-\alpha^2}} \sqrt{\frac{1+\sqrt{1-\alpha^2}}{\Gamma(1+2\sqrt{1-\alpha^2})}} \begin{pmatrix} 1 \\ 0 \\ \frac{\alpha}{1+\sqrt{1-\alpha^2}} \begin{pmatrix} i \cos \theta \\ i e^{i\phi} \sin \theta \end{pmatrix} \end{pmatrix}$$

Direct inspection of the Schrodinger and Dirac ground state solutions immediately reveals serious problems with both solutions. In the Schrodinger case, the $e^{-\frac{r}{a_0}}$ term leads to a cusp at the origin, as shown in Figure 2. In the Dirac case, the $\left(\frac{2r}{a_0}\right)^{-1+\sqrt{1-\alpha^2}}$ term has a very small negative exponent, leading to a singularity at the origin, as pointed out by Darwin in 1928, and reiterated by Itzykson and Zuber (1980, p. 79).

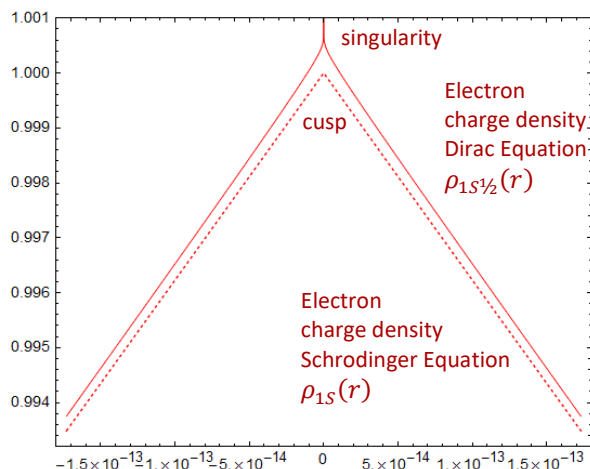


Figure 2: (a) Electron Charge Density for the Dirac Equation (singular) and Schrodinger Equation (cusp). Neither of these well-known solutions are physically plausible near the origin.

The Schrodinger and Dirac Hydrogen wavefunction solutions are foundational in modern physics education, but neither of these solutions are physically plausible, nor qualitatively or quantitatively correct, near the origin. The QED literature corrects the energy levels but never shows how the wavefunctions are affected.

The usual way to find the wavefunction, given a proposed modified potential, would be to use Perturbation Analysis. However, since the problem is stiff, i.e., there are two very different spatial dimensions (the Bohr radius and the Compton radius), we found that Perturbation Analysis did not converge. Therefore, to find the correct behavior, we must use a Numerical method to find a Dirac solution with a properly modified potential.

4. Numerical Solution for Modified Dirac Wavefunction

Hammerling et al. (2010) has developed a set of procedures for numerical solution of singular eigenvalue problems on semi-infinite domains, with emphasis on Sturm-Liouville problems in general, and with the time-independent Schrödinger equation for a central potential as a particular example. Their standard approach is to truncate to a bounded interval, start with an initial educated guess of the eigenvalue (energy) and use a *two-sided shooting method*, integrating from $r = 0$ outward, and from $r = r_{max}$ inward, and adapting the eigenvalue until the two integrated halves match in value and derivatives at an intermediate point, leading to an energy value and a complete, continuous function that satisfies the differential equation and both boundary conditions. We implemented this type of method for the Schrodinger case, and adapted it to the more difficult Dirac case.

4.1. Energy and Electron Wavefunction for the $1S^{1/2}$ state

For the $1S^{1/2}$ state, the next step is to compute the new energy and electron wavefunction corresponding to this modified Coulomb potential $V_{1S^{1/2}}(r)$. We will first set up the problem, and then show the various methods we have used to solve the problem.

The energy level of the unmodified $1S^{1/2}$ ground state is

$$E_{1S^{1/2}} = mc^2 \sqrt{1 - \alpha^2}.$$

Note that the relativistic energy includes the rest mass mc^2 which must be subtracted away before it can be compared to the non-relativistic energy. Because we have made a modification to the potential near the origin, we should expect that there should be a small change in the energy for a self-consistent wavefunction solution. Let us define the modified energy $E_{1S^{1/2}m}$ as a tiny fractional change to the original energy with the rest mass removed:

$$\begin{aligned} E_{1S^{1/2}m} &= (E_{1S^{1/2}} - mc^2)(1 + \varepsilon_{1S^{1/2}}) + mc^2 \\ &= mc^2 \left(1 + (-1 + \sqrt{1 - \alpha^2})(1 + \varepsilon_{1S^{1/2}}) \right) \\ &= mc^2 \left(\sqrt{1 - \alpha^2} + \varepsilon_{1S^{1/2}}(-1 + \sqrt{1 - \alpha^2}) \right) \end{aligned}$$

where $\varepsilon_{1S^{1/2}}$ is a small, dimensionless quantity. With this definition, we can expect an approximate value of $\varepsilon_{1S^{1/2}} \approx -\frac{1}{1,000,000}$ as in the non-relativistic case.

Substituting the previous expressions for $E_{1S^{1/2}m}$ and $V_{1S^{1/2}}(r)$ for the Gaussian Charge Distribution assumption leads to the Modified Ground State Equation (along with its boundary conditions and the charge normalization condition):

$$\begin{aligned} f_{1S^{1/2}m}'(r) - \left(\frac{1 + \sqrt{1 - \alpha^2} + \varepsilon_{1S^{1/2}}(-1 + \sqrt{1 - \alpha^2})}{\alpha a_0} + \frac{\alpha}{r} A_{1S^{1/2}}(r) \right) g_{1S^{1/2}m}(r) &= 0 \\ g_{1S^{1/2}m}'(r) + \frac{2}{r} g_{1S^{1/2}m}(r) + \left(\frac{-1 + \sqrt{1 - \alpha^2} + \varepsilon_{1S^{1/2}}(-1 + \sqrt{1 - \alpha^2})}{\alpha a_0} + \frac{\alpha}{r} A_{1S^{1/2}}(r) \right) f_{1S^{1/2}m}(r) &= 0 \\ A_{1S^{1/2}}(r) &= \frac{V_{1S^{1/2}}(r)}{V(r)} = \text{Erf} \left(\frac{r}{\sqrt{2} r_Z} \right) \\ f_{1S^{1/2}m}(\infty) &= 0 \\ g_{1S^{1/2}m}(\infty) &= 0 \\ \int_0^\infty (f_{1S^{1/2}m}(r)^2 + g_{1S^{1/2}m}(r)^2) r^2 dr &= 1 \end{aligned}$$

And the challenge is to solve for the fractional energy change $\varepsilon_{1S^{1/2}}$ and the wavefunctions $f_{1S^{1/2}m}(r)$ and $g_{1S^{1/2}m}(r)$.

4.1.1. Numerical solution for the $1S^{1/2}$ state

We use the two-sided shooting method, adapted to the specific needs of the Relativistic case, with the coupled equations for $f_{1S^{1/2}m}(r)$ and $g_{1S^{1/2}m}(r)$, similar to Silbar et al. (2010). The solution will be determined by $\varepsilon_{1S^{1/2}}$ and the two additional free parameters

$$\text{gfratio}(r_{min}) = \frac{g_{1S^{1/2}m}(r_{min})}{f_{1S^{1/2}m}(r_{min})}, \quad \text{gfratio}(r_{max}) = \frac{g_{1S^{1/2}m}(r_{max})}{f_{1S^{1/2}m}(r_{max})}$$

For the original Dirac solution,

$$\text{gfratio}(r_{min}) = \text{gfratio}(r_{max}) = -\frac{\alpha}{1 + \sqrt{1 - \alpha^2}}$$

Early experiments with the numerical solution of the Modified Ground State equations led directly to

$$\text{gfratio}(r_{min}) = 0, \quad \text{gfratio}(r_{max}) = -\frac{\alpha}{1 + \sqrt{1 - \alpha^2}}$$

as promising initial values, subject to joint optimization along with $\varepsilon_{1S^{1/2}}$. This problem can be solved numerically using the following procedure:

1. **Goal of the procedure:** The procedure is designed to solve for $\varepsilon_{1S^{1/2}}$, $\text{gfratio}(r_{min})$, and $\text{gfratio}(r_{max})$.
2. **Initialization:** Choose an initial value for ε_1 : We used -1.0×10^{-6} . Choose initial values $\text{gfratio}(r_{min}) = 0$, $\text{gfratio}(r_{max}) = -\frac{\alpha}{1 + \sqrt{1 - \alpha^2}}$, where we defined $r_{max} = 30r_c$ and $r_{min} = \frac{r_{max}}{1000000000}$. We will also need two midpoints for continuity matching: we used $r_{mid1} = 11r_c$ and $r_{mid2} = 40r_c$.
3. **“Outward” and “Inward” shooting integrations:** Define the interval in which to perform the outward shooting-method integration for r running from r_{min} to r_{mid2} . Define the interval in which to perform the inward shooting-method integration for r running from r_{max} to r_{mid1} . Note that the two integrations overlap on the interval r_{mid1} to r_{mid2} . The integrations can be done directly in Mathematica by **NDSolve**. Each integration will produce trial wavefunctions $f_{1S^{1/2}m}(r)$ and $g_{1S^{1/2}m}(r)$.
4. **Continuity and Charge Normalization Condition:** We now have a trial “outward” and “inward” numerical integrations done. We scale the “inward” solution so that the “inward” $f_{1S^{1/2}m}(r)$ agrees with the “outward” $f_{1S^{1/2}m}(r)$. We then numerically compute the charge normalization integral, using the “outward” solution from r_{min} to r_{mid1} , and the “inward” solution from r_{mid1} to r_{max} , and then scale the composite solution to normalize the charge. At this point, we have a two-part normalized solution where the “inward” and “outward” parts match at $f_{1S^{1/2}m}(r_{mid1})$, but may not match at $g_{1S^{1/2}m}(r_{mid1})$, $f_{1S^{1/2}m}(r_{mid2})$, and $g_{1S^{1/2}m}(r_{mid2})$. To match these three additional conditions, we may need to adjust $\varepsilon_{1S^{1/2}}$, $\text{gfratio}(r_{min})$, and $\text{gfratio}(r_{max})$.
5. **Inner Loop Iteration Condition:** We defined the difference solutions as the deviation between the modified solutions and the corresponding original Dirac solution:

$$f_{1S^{1/2}d}(r) = f_{1S^{1/2}m}(r) - f_{1S^{1/2}}(r)$$

$$g_{1S^{1/2}d}(r) = g_{1S^{1/2}m}(r) - g_{1S^{1/2}}(r)$$

and the Error as

$$\begin{aligned} \text{Error} = & \left(g_{1S^{1/2}doutward}(r_{mid1}) - g_{1S^{1/2}dinward}(r_{mid1}) \right)^2 \\ & + \left(f_{1S^{1/2}doutward}(r_{mid2}) - f_{1S^{1/2}dinward}(r_{mid2}) \right)^2 \\ & + \left(g_{1S^{1/2}doutward}(r_{mid2}) - g_{1S^{1/2}dinward}(r_{mid2}) \right)^2 \end{aligned}$$

which will vanish when the continuity condition is met, i.e., the “outward” and “inward” integrations agree, in both the f and g terms, at both points r_{mid1} and r_{mid2} . Holding $\text{gfratio}(r_{min}) = 0$ and $\text{gfratio}(r_{max}) = 1$ constant, we used Mathematica’s **NDSolve** to find the minimum value of Error as a function of $\varepsilon_{1S^{1/2}}$. We found the Minimum Error of 5.05×10^{-19} at $\varepsilon_{1S^{1/2}} = -2.5424935 \times 10^{-6}$. Since the value of the Minimum Error is so close to zero, we concluded that the initial values of $\text{gfratio}(r_{min})$ and $\text{gfratio}(r_{max})$ needed no further modification to find a completely self-consistent solution.

The original Dirac electron charge density is given by

$$\rho_{1S^{1/2}}(r) = q \frac{(f_{1S^{1/2}}(r))^2 + (g_{1S^{1/2}}(r))^2}{4\pi}.$$

The modified electron charge density is given by

$$\rho_{1S^{1/2}m}(r) = q \frac{(f_{1S^{1/2}m}(r))^2 + (g_{1S^{1/2}m}(r))^2}{4\pi}.$$

The difference electron charge density is given by

$$\rho_{1S^{1/2}d}(r) = \rho_{1S^{1/2}m}(r) - \rho_{1S^{1/2}}(r).$$

These charge densities are shown in Figure 3, illustrating that, relative to the original Dirac Solution, charge is displaced outward from the origin as in the non-relativistic case, and the singularity in the Original Dirac charge density is eliminated, in favor of a well-behaved “rounded top”.

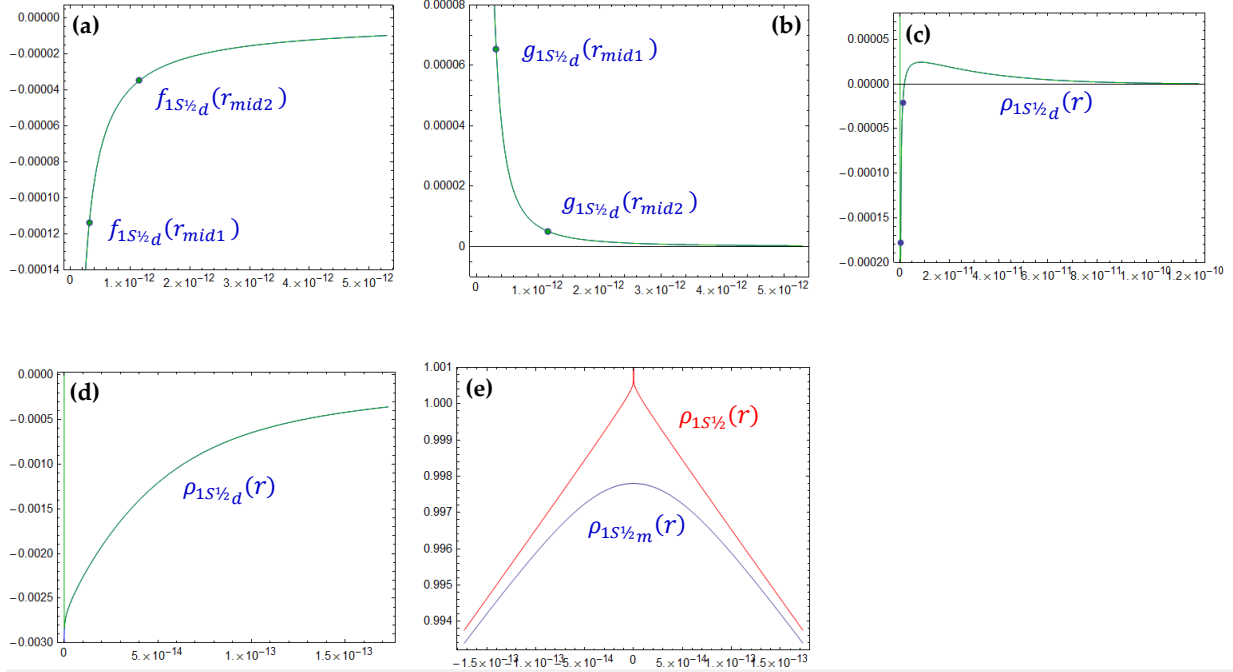


Figure 3: Continuity conditions for the $1S^{1/2}$ numerical solution. (a) “Outward” (blue) and “Inward” (green) $f_{1S^{1/2}_d}(r)$ difference solutions, matching at r_{mid1} and r_{mid2} , which results in them matching everywhere. (b) “Outward” (blue) and “Inward” (green) $g_{1S^{1/2}_d}(r)$ difference solutions, matching at r_{mid1} and r_{mid2} . (c) Corresponding Electron charge density differences from the original Dirac Solution, showing that charge lost near the origin is displaced outward from the origin, as in the non-relativistic case. (d) Detailed view of the Electron charge density deviations from the original Dirac Solution near the origin. (e) Comparison of the Original Dirac Electron charge density, which has a singularity at the origin, to the modified charge density, which has the expected “rounded top” with no singularity.

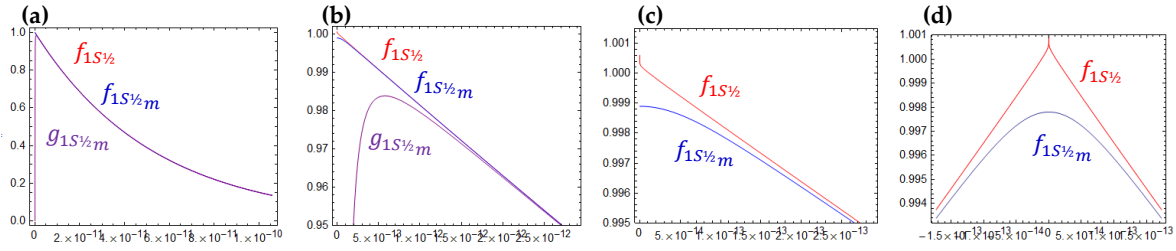


Figure 4: The modified $f_{1S^{1/2}_m}$ and scaled $g_{1S^{1/2}_m}$ solutions, along with the original $f_{1S^{1/2}}$ solution, at a variety of different scales. (a) At this scale, we see the broadly exponential behavior of $f_{1S^{1/2}_m}$ and $f_{1S^{1/2}}$, and we see that $g_{1S^{1/2}_m}$ is driven to zero near the origin. (b) At this scale, we see the slight modification of $f_{1S^{1/2}_m}$ relative to $f_{1S^{1/2}}$ near the origin, and the large modification of $g_{1S^{1/2}_m}$ near the origin. (c,d): At these scales, we see further detail of the “rounded-top” behavior of $f_{1S^{1/2}_m}$ relative to $f_{1S^{1/2}}$ near the origin.

We have similarly performed the numerical analysis for the $2S_{1/2}$ solution of the Dirac Hydrogen Atom with the modified Coulomb potential for the Sub-Compton Gaussian Charge Distribution case, and we see very similar behavior as shown in Figure 5.

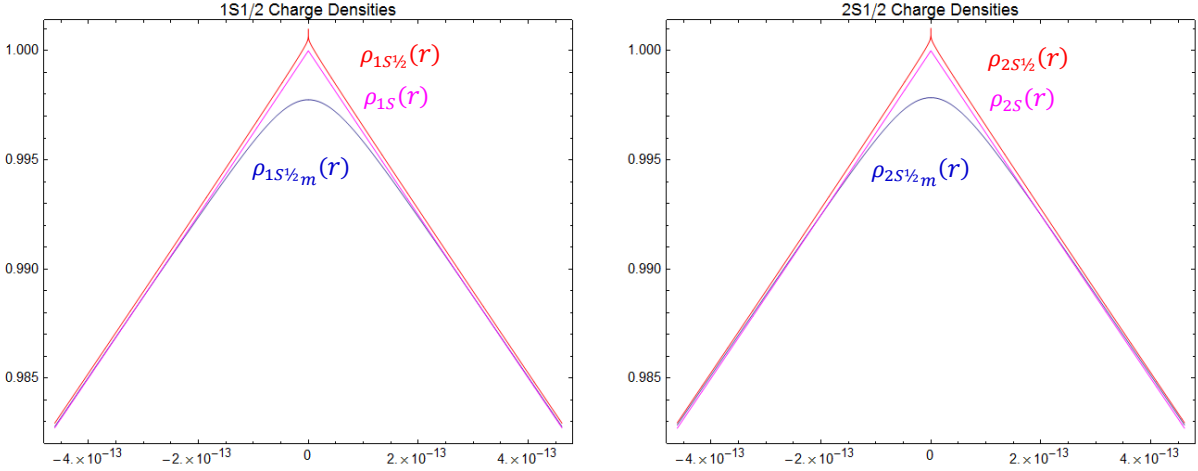


Figure 5: Summary of original Dirac charge probability density (red), Schrodinger charge probability density (magenta) and revised charge probability density plots for the Gaussian Charge Distribution case (blue). The modified charge probability densities correspond to the correct energy shifts matching the Lamb Shift data and modern QED theory. Note that the original Dirac charge probability density is singular at the origin, and the Schrodinger charge probability density has a cusp at the origin; the modified charge probability density has a well-behaved “rounded top” at the origin.

The composite numerical/analytic wavefunction solution is difficult to visualize in a single picture because the “stiff” nature of the problem gives the solution features on very short (r_c) and on very long (a_0) spatial scales. We will describe the general features using a conceptual but not-to-scale diagram in Figure 4 to illustrate how the charge is redistributed relative to the familiar Schrodinger solution.

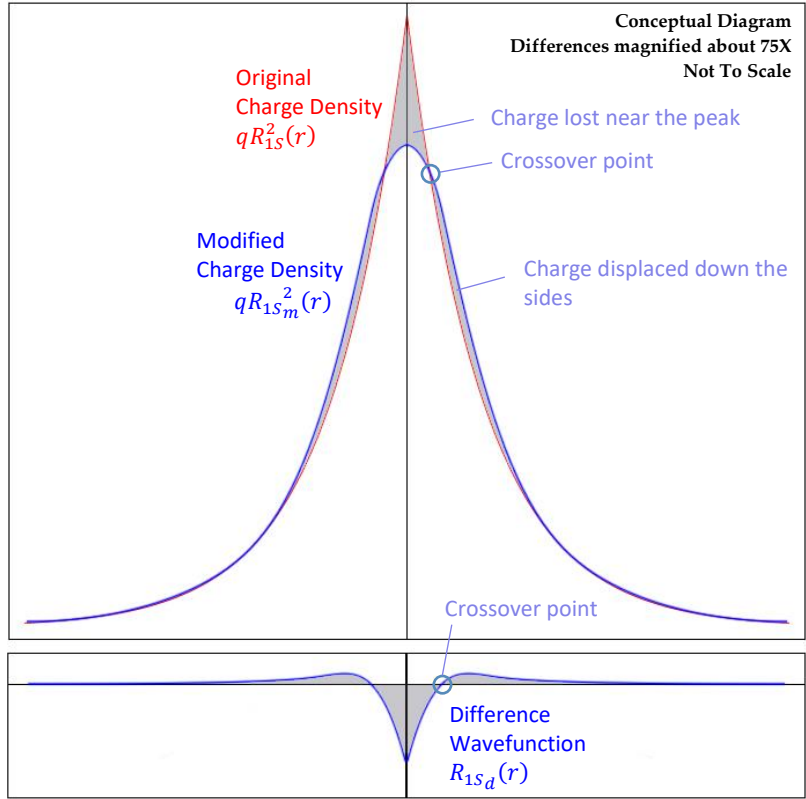


Figure 6: Conceptual diagram (not to scale) showing the general features of the modified ground state wavefunction $R_{1S_m}(r)$, with reference to the original ground state wavefunction $R_{1S}(r)$. The difference wavefunction $R_{1S_d}(r)$ is shown in the lower panel. Differences have been magnified about 75X to show general features.

The original wavefunction $R_{1S}(r)$ has a cusp at $r = 0$. The modified wavefunction $R_{1S_m}(r)$ has a “rounded top” at a lower amplitude value, indicating that some charge has been lost near the origin. At the crossover point, the modified wavefunction becomes larger than the original wavefunction, indicating that some charge has been displaced down the sides of the distribution. The same charge displacement features appear in the difference wavefunction $R_{1S_d}(r)$ in the lower panel.

In other work (not detailed here) we have developed closed-form approximations to the modified Hydrogen wavefunction and charge densities, in terms of Confluent Hypergeometric Functions. This work may appear in a subsequent publication.

We have computed the Hydrogen wavefunctions and charge probability density functions for the Exponential Charge distribution assumption and found the results to be qualitatively similar to the Gaussian case, i.e. well-behaved, rounded top, small component driven to zero near the origin, and no singularity or cusp at the origin. We expect similar behavior for the other two distributions.

5. Implications for a Free Electron

Existing QED theory for the leading (non-relativistic) term of the Lamb Shift is

$$\Delta E_{<} = mc^2 \frac{4}{3\pi} \frac{(Z\alpha)^4 \alpha}{n^3} \ln \left(\frac{mc^2}{k_0(n, l)} \right)$$

where $\ln k_0(n, l)$ is the Bethe Logarithm, which has been tabulated (Jentschura and Mohr, 2005) for the commonly used values of n and l .

| n | $\ln \frac{k_0(n, 0)}{\text{Ry}}$ | $\ln \frac{k_0(n, 1)}{\text{Ry}}$ |
|----------|---|---|
| 1 | 2.984129 | --- |
| 2 | 2.811770 | -0.0300167 |
| 3 | 2.767664 | -0.0381902 |
| 4 | 2.749812 | -0.0419549 |
| 20 | 2.723967 | -0.0486082 |
| 200 | 2.722668 | -0.0490495 |
| ∞ | 2.722654 | -0.0490545 |

Table 3. Bethe Logarithms. The highlighted values (2S, 2P) are used in the Lamb Shift calculation.

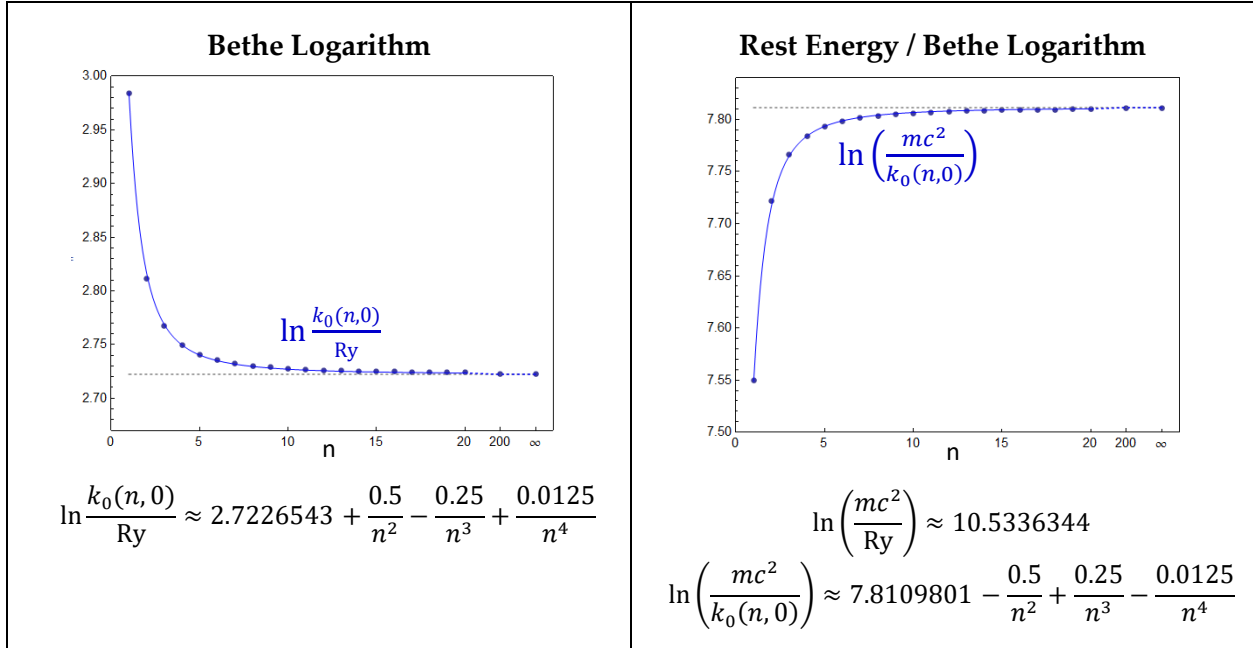


Figure 4. Bethe Logarithms in different useful forms.

For our purposes, it is most convenient to use a series approximation for the Rest Energy / Bethe Logarithm ratio:

$$\Delta E_{<} = mc^2 \frac{4}{3\pi} \frac{(Z\alpha)^4 \alpha}{n^3} \left(7.8109801 - \frac{0.5}{n^2} + \frac{0.25}{n^3} - \frac{0.0125}{n^4} \right)$$

which shows the usual $\frac{1}{n^3}$ dependence, along with the $\ln\left(\frac{mc^2}{K_0(n,l)}\right)$ term, which deviates from its asymptotic value of 7.8109801 by at most 3.3%.

The $\frac{1}{n^3}$ dependence captures the strong effect of the principal quantum number on the Lamb Shift, which is much larger for small n because of the density of the wavefunction at the origin for the S states, which becomes much less dense for large n . We interpret the $\ln\left(\frac{mc^2}{K_0(n,l)}\right)$ term as related to the size of the electron's charge distribution, and this term is largely constant with n , but has a small (3.3%) compression for the smallest values of n , relative to the asymptotic value, which we interpret as related to the free electron case. Therefore, we believe that the conclusions we draw about the size of the electron's charge distribution from the low- n bound states will closely apply to the free electron case, within a few percent. The Lamb Shift from bound states tells us within a few percent the size of the free electron charge distribution. (Note that this assumes that a free electron behaves like an electron in a bound S state with $n = \infty$. If this assumption is incorrect, we could instead have an error as large as $\frac{10.53-7.55}{7.81} = 38.2\%$).

So far, we have several proposed charge distributions, each of which must be tightly localized within the half-Reduced Compton Wavelength, but no way yet of preferring one over the others. We can see two ways to try to determine the correct charge distribution:

1. Derive the charge distribution from direct knowledge of the components of the Bethe Logarithm. Such an approach would directly tie the QED derivation of the Lamb Shift to the detailed form of the charge distribution. We believe this would require cooperation, collaboration, or support from physicists who have the existing knowledge and software tools to analyze the Bethe Logarithm components, i.e. Jentschura and Mohr.
2. Another way to choose would be to look for stability and persistence of the candidate charge distributions. A stable charge distribution that persists over time in the free electron case would be a greatly stronger candidate than one that dissipates over time.

In the following section 6, we attempt direct numerical simulation of 3D Dirac Equation in Free Space, with different initial conditions (Sub-Compton Gaussian, or Sub-Compton Spherical Shell), to see if they lead to stable charge distributions.

6. Free Electron Numerical Simulations – Prior 1D, 2D

Thaller [2005] has provided a Mathematica Toolbox for simulations and visualizations of the Dirac Equation, and a set of QuickTime animations for the 1D and 2D cases. He focuses on Gaussian Wavepacket initial conditions for a Free Electron, showing how those states evolve over time. And he gives examples of positive-energy initial conditions, which do not exhibit Zitterbewegung, and mixed-energy initial conditions, which do exhibit Zitterbewegung. The key relevant examples are shown in Figures 3 and 4.

The key messages from these figures are:

- Gaussian distributions disperse. If they are not initially tightly localized (Fat initial distributions), they disperse slowly. If they are initially tightly localized (Narrow initial distributions), they disperse with shock fronts moving at the speed of light.
- Positive-only initial distributions do not exhibit Zitterbewegung.
- Mixtures of positive and negative energy states exhibit Zitterbewegung – jittering motion, both in the mean position vs. time, and in the wobbly, ripply behavior of the Wavepacket envelope as it spreads.
- The dispersion in the 2D case takes the form of an initial Gaussian spreading out in a ring, much like the outward surface wave from a pebble dropped in a pond. In the first 2D example given by Thaller, a positive-energy initial condition is used, and the wavefront envelope spreads out with circular symmetry. In the second example, a mixed-energy initial condition is used, and the wavefront envelope spirals outward, in an expanding and spinning motion.

6.1.1D

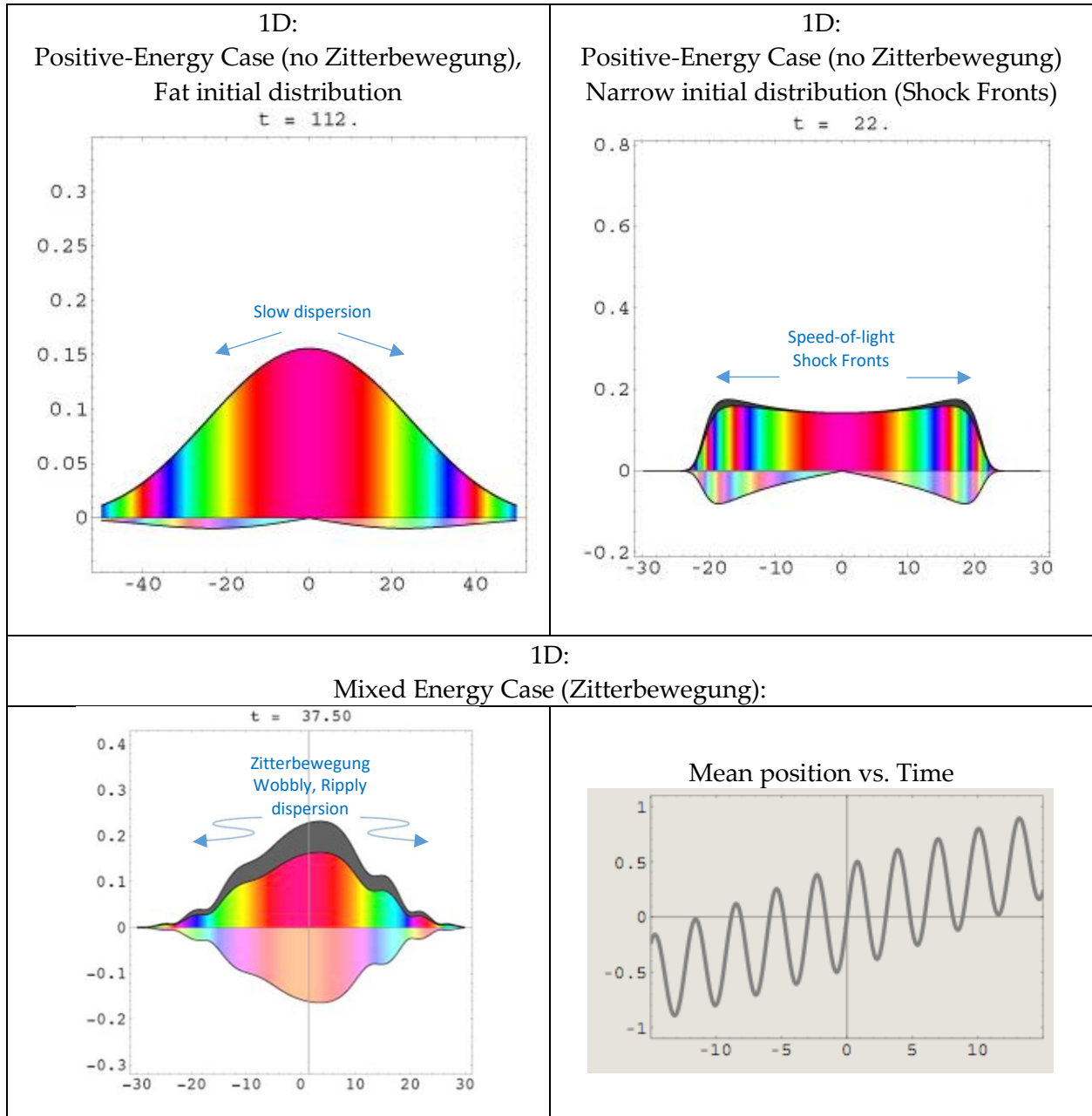


Figure 3. Time evolution of Gaussian Wavepackets for the Dirac Equation (1D case).
The x-axis is distance in units of λ_C .

6.2.2D

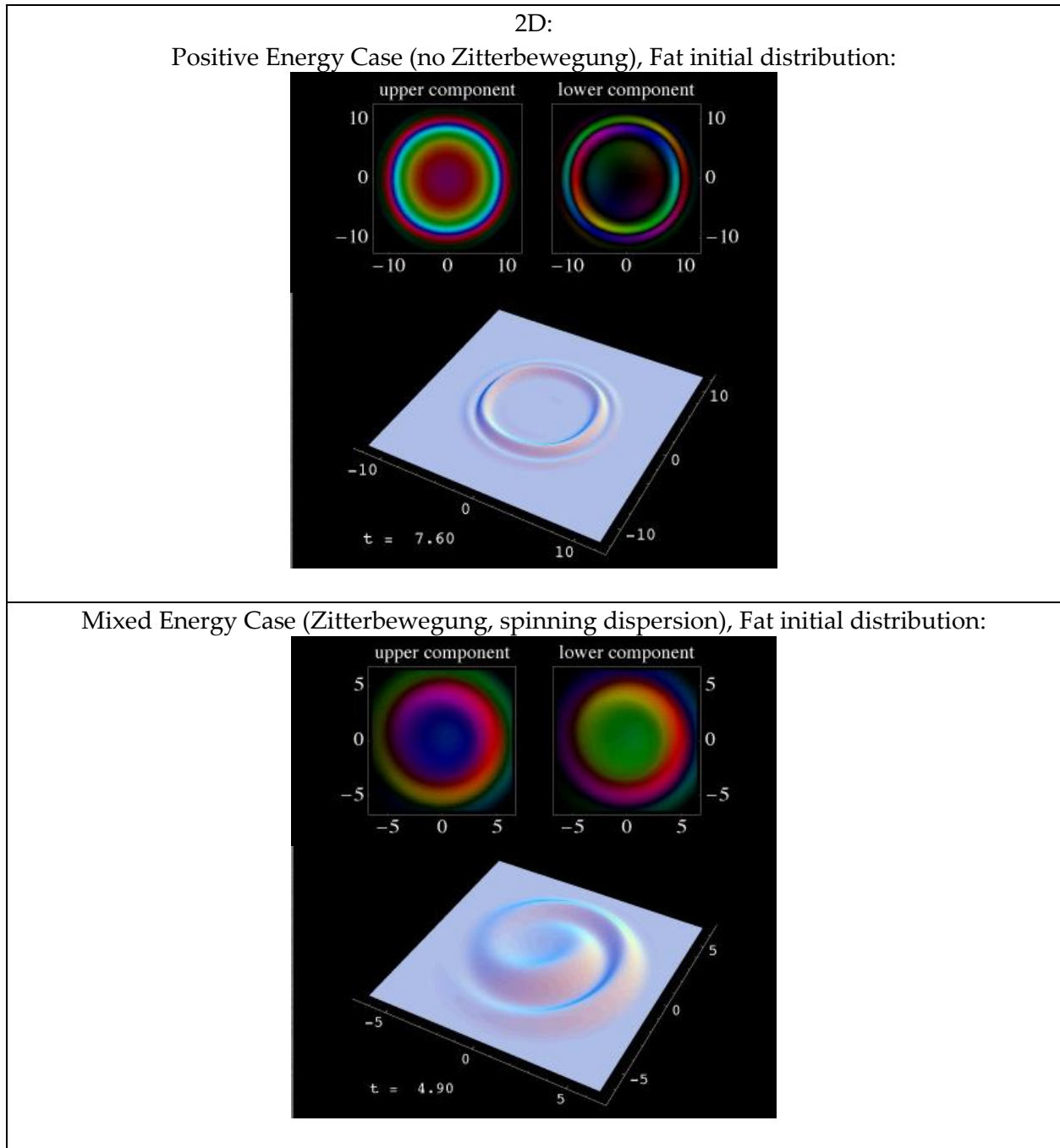


Figure 4. Time evolution of Gaussian Wavepackets for the Dirac Equation (2D case).

Thaller presents these as illustrative behaviors of the Dirac Equation in 1D and 2D. But he doesn't give 3D examples, and he doesn't discuss the physical implications of the dispersion. At face value, these illustrations would seem to suggest that an electron (as represented by a Gaussian Wavepacket in the Dirac Equation in 1D and 2D) is unstable – it disperses until it is everywhere.

7. Free Electron Numerical Simulations – New 1D, 2D, 3D

The previous analysis suggested that we are looking for a stable charge distribution that fits within a Reduced Compton Wavelength in 3D. In Thaller's terms, this would correspond to a 3D Dirac Equation simulation with positive-only energies, highly confined (initial distribution entirely inside radius of a Half-Reduced Compton Wavelength). Thaller did not do this simulation. His closest examples were 1D Narrow, or 2D Fat, but nothing like 3D Super-Narrow. It is possible that there is a surprise waiting in the numerical simulations that no-one has anticipated based on analytical reasoning. So the next steps would appear to be to do the 3D Dirac Equation numerical simulations for the Super-Narrow case.

A best case result would be that an initial very tight Gaussian distribution would disperse outward in a 3D wavefront (shock front) until it reaches a spherical shell of radius (approximately) $r_z \approx \frac{\lambda_c}{2} (0.38126)$, and then stabilizes at that distribution, finding a kind of stable attractor. If the numerical simulations showed this, it would be a remarkable numerical result, and would justify looking for an analytic explanation of the phenomenon.

Another way to begin would be to try to construct a Charged Shell initial condition and determine what conditions lead to its stability.

If a stable shell-like solution is not found, we might then wonder if there is something missing from the Dirac equation (an additional term, or a nonlinearity of some kind) that would provide the additional stabilizing factor at the correct radius.

7.1. 1D Super-Narrow

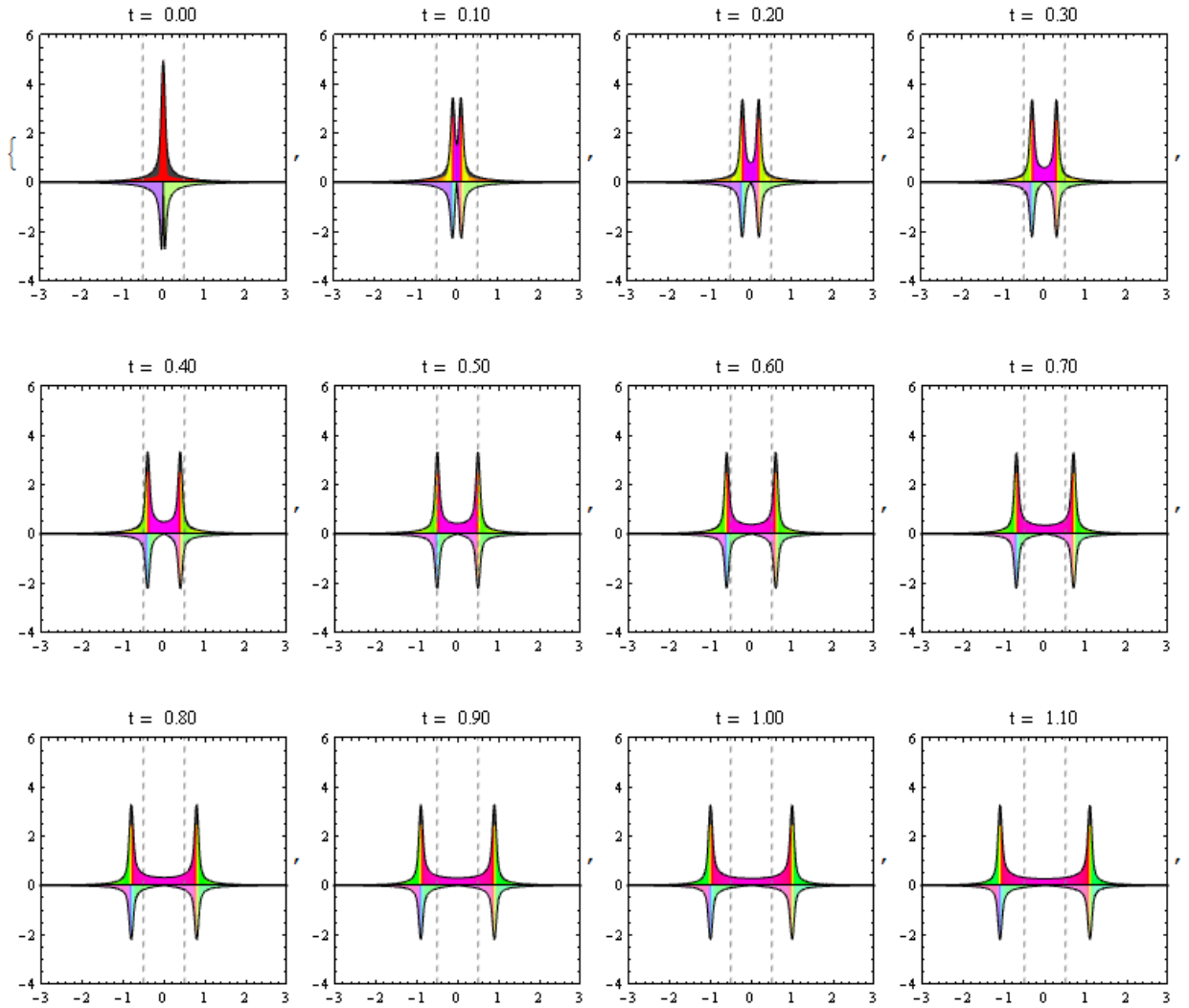


Figure 5. Time evolution of Super-Narrow Initial Gaussian-like Wavepacket for the Dirac Equation (1D case). The Gray Dashed lines indicate $\pm \frac{\lambda_c}{2}$.

This example looks as would be expected: a Super-Narrow initial distribution, effectively contained inside the Reduced Compton Wavelength, leads to a rapidly expanding Shock Fronts moving in both directions outward from the origin at the speed of light.

7.2. 2D Super-Narrow

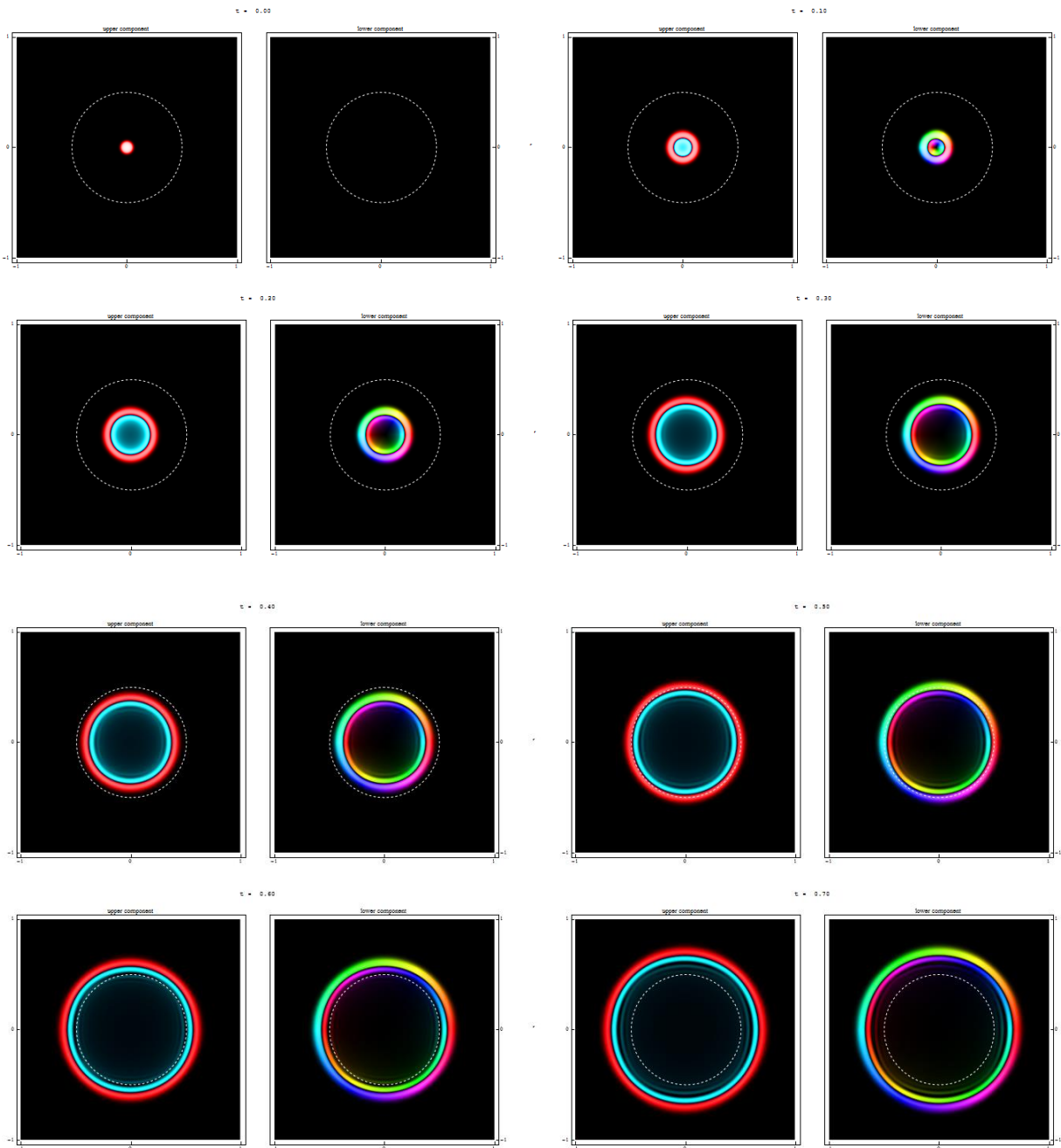


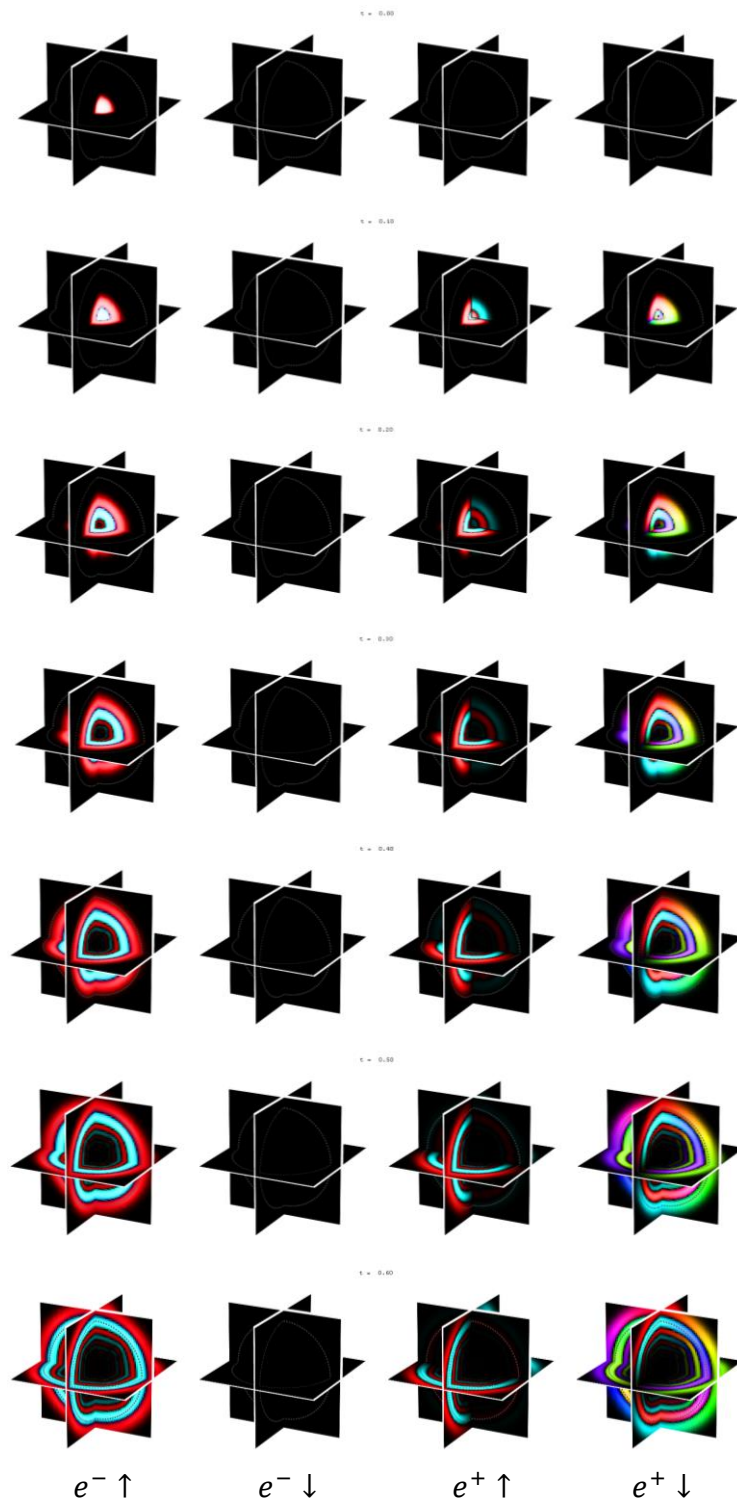
Figure 6. Time evolution of Super-Narrow Initial Gaussian-like Wavepacket for the Dirac Equation (2D case). The Gray Dashed circle has radius of $\frac{\lambda_C}{2}$.

This example looks as would be expected: a Super-Narrow initial distribution, effectively contained inside the Reduced Compton Wavelength, leads to a rapidly expanding 2D radial Shock Fronts moving outward from the origin at the speed of light.

How to display a 3D complex variable? For a 3D Dirac equation simulation, we will need 4 of them, one for each wavefunction component. For each one, we will show three orthogonal cross-sections going through the origin, so we can see internal structure. The four components are

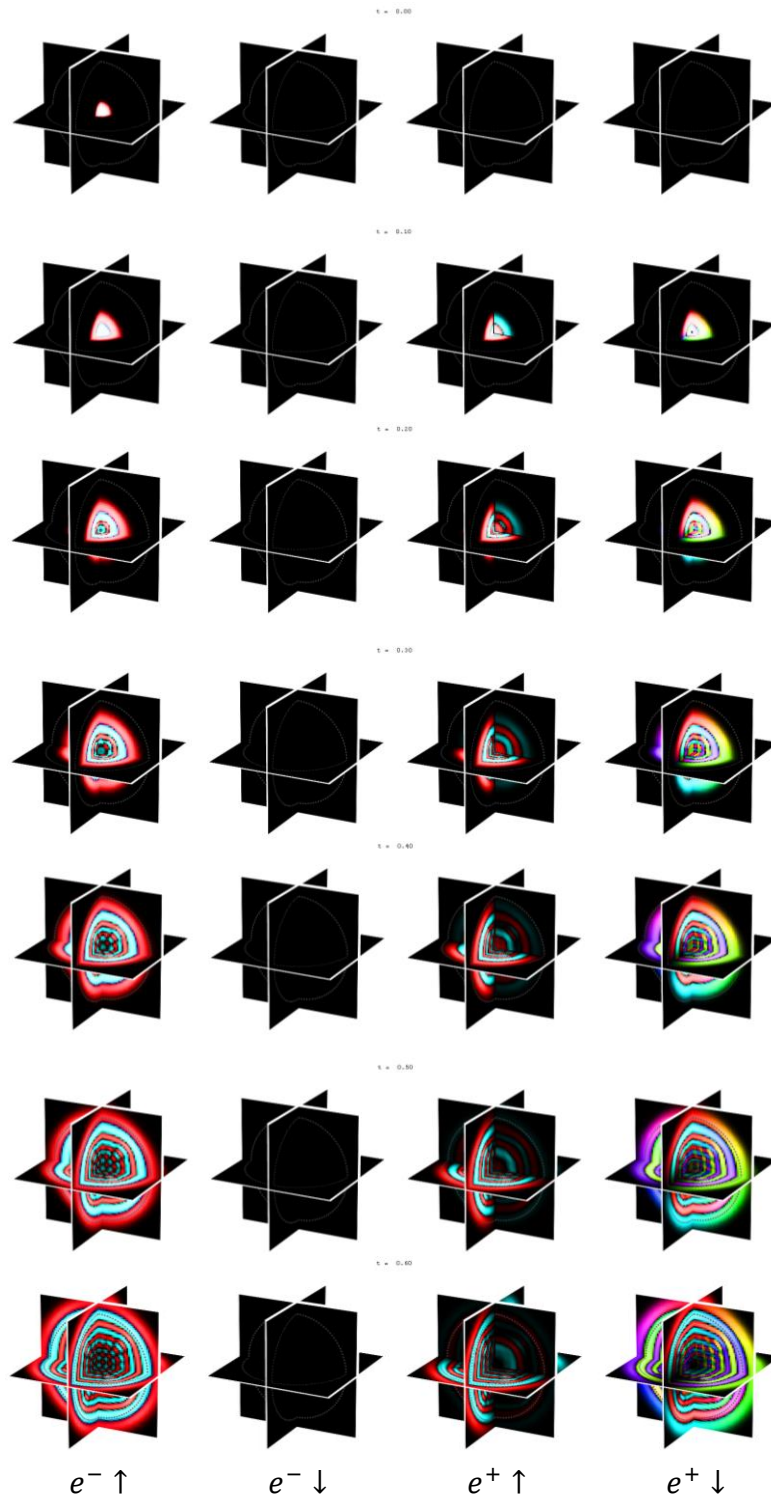
- Positive Energy, Electron, Spin Up ($e^- \uparrow$)
- Positive Energy, Electron, Spin Down ($e^- \downarrow$)
- Negative Energy, Positron, Spin Up ($e^+ \uparrow$)
- Negative Energy, Positron, Spin Down ($e^+ \downarrow$).

7.3. 3D Tight Gaussian

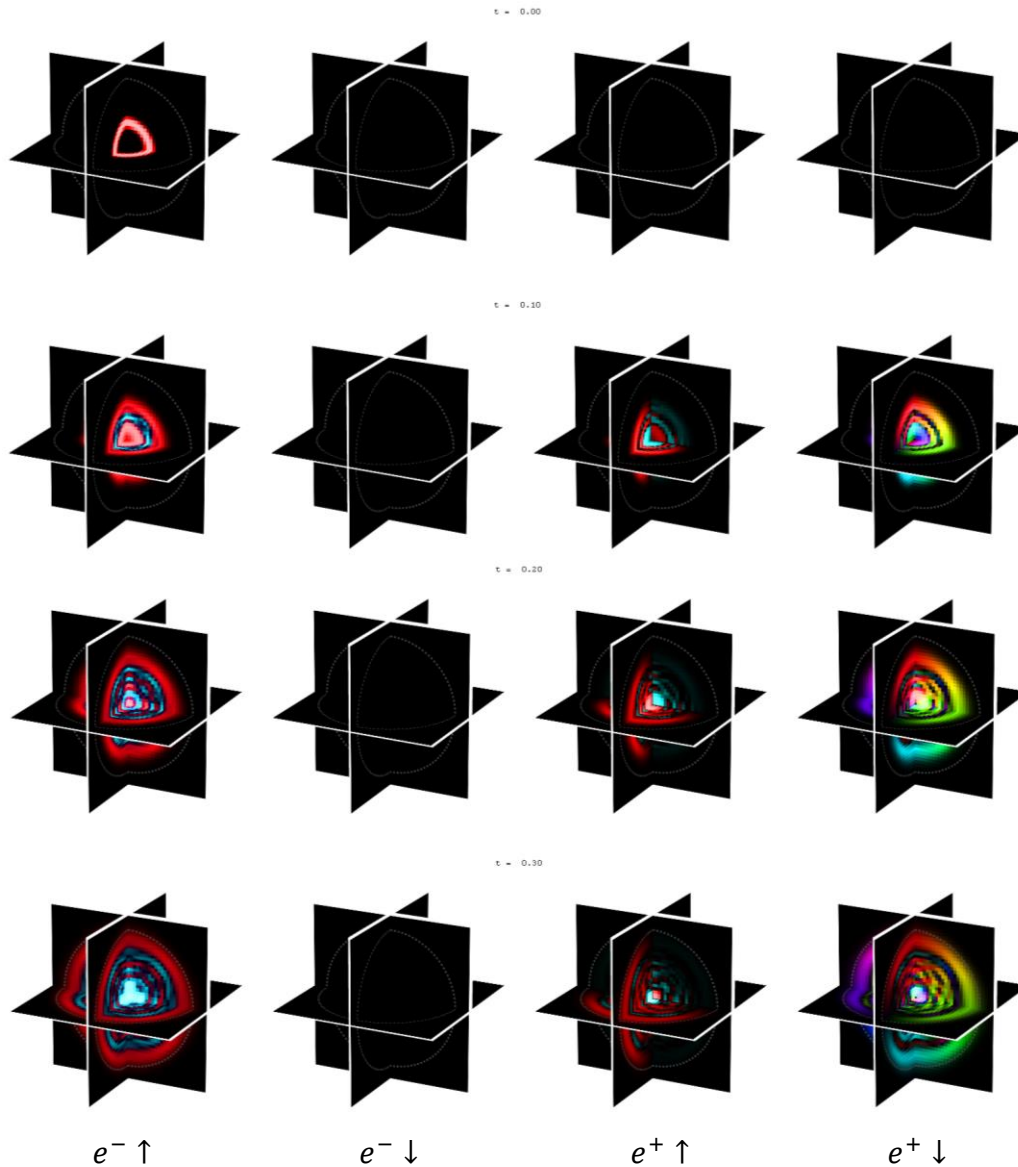


It does not show any signs of a stable configuration, it seems to be continually expanding outside the Half-Reduced Compton Radius. It does seem that the thinner the initial Gaussian distribution, the thinner are the “layers” of the outward-moving ripples.

7.4.3D Very Tight Gaussian



7.5. 3D Spherical Shell



It still creates an outgoing (and ingoing) wave, regardless of whether or not there is charge. So, we will conclude that the Dirac Equation does not lead to a stable constrained charge distribution.

8. Modifying the Dirac Equation to get a Stable Configuration

It appears that the Dirac equation, on its own, does not produce a stable constrained distribution, at least for the few conditions we tried. This is to be expected; the charge spreading is a QED effect, which is not an inherent part of the Dirac Equation. Below are some highly speculative notes about how the Dirac Equation might be modified to take the QED charge-spreading effect into account.

Some additional constraint, or nonlinearity, or term, is needed to be added to the Dirac equation to create a stable constrained distribution.

If the Upper Component is the positive energy component (electron), and the Lower Component is the negative energy component (positron), could that introduce an additional attractive force that has not been taken into account (Dirac equation does not include Charge!)?

Dirac Equation comes from the combination of Quantum Mechanics and the Energy-Momentum Relation of Special Relativity. But this assumes that the electron is not experiencing accelerated motion, which is clearly a very poor assumption when the electron is very close to the nucleus of the atom. This also suggests that the Dirac Equation would require some modification to account for the acceleration it experiences near the nucleus of the atom. Could it be that some kind of General Relativity term is needed, not to account for acceleration due to gravitational attraction, but to account for acceleration due to electromagnetic attraction?

9. Discussion

We have shown that four different sub-Compton charge density proposals can be made consistent with the Lamb Shift. But which one (if any) of them is right? Recall that each proposal was based on a unique physical model, derived from some plausible mechanism, by credible relativistic physicists. We have made a proposal that the correct distribution could be derived from knowledge of the higher-order moments (Bethe Logarithm components), with the hard work still to be done. If this work could be completed, we would have a definitive description of the sub-Compton charge density of the electron. The importance of this cannot be overstated. It would give us a deep insight into an underlying physical behavior of the electron at sub-Compton scales. Quantum Electrodynamics can make the statement that the electron “continuously emits and absorbs virtual photons, and as a result its electric charge is spread over a finite volume instead of being pointlike.” [Eides, Grotch, and Shelyuto, 2007] But it does not tell us *how* the charge is spread, what shape, what motion, what wavefunction? With the higher-order moments of the Bethe Logarithm, we may be in a position to answer the question definitively, or at least significantly constrain the options.

We will speculate briefly on the choices, to illustrate how significant it would be to have a definitive answer.

1. If it should turn out that the Charged-Shell Distribution inspired by Hestenes' Space-Time Algebra were supported by the higher-order moments calculation, it would provide external validation to Hestenes' helical motion / Zitterbewegung proposal. It would give deep insight into the connection between the “continuous emission and absorption of

virtual photons” and the spin of the electron, by confirming that the electron “at rest” is really moving in a circular path in three dimensions.

2. If it should turn out that the Imaginary Charged-Ring Distribution inspired by Barut and Bracken’s Zitterbewegung analysis were supported by the higher-order moments calculation, it would provide external validation to Barut and Bracken’s relativistic analysis. It would give deep insights into the connection between the “continuous emission and absorption of virtual photons” and the spin of the electron, by confirming that the electron “at rest” is really moving in a circular path in two auxiliary dimensions.
3. If it should turn out that the Exponential Distribution were supported by the higher-order moments calculation, it would provide external validation to the idea that the small component acts like a “mini-positron”, creating some kind of sub-orbital system from the large and small components. This idea would have further implications for the origin of electron spin.
4. If it should turn out that the Gaussian Distribution were supported by the higher-order moments calculation, it could provide external validation to the idea that the underlying physics of the electron is dominated by some random process (like Bracken’s Quantum Random Walk) or Brownian-like motion, i.e. the electron is randomly jittering, not moving in a circular or orbital path. Or there could be some other underlying physics that could lead to a Gaussian Distribution. From Carver Mead [personal communication]: “I don't believe there is any randomness in the spread of the wave function itself. And a Gaussian, to me, says nothing that would imply randomness. It is a perfectly good shape for the square of the amplitude of a totally coherent standing wave. In that case it would be telling us something about the "effective potential" of the electron-proton pair. This is not to say that every Hydrogen atom is in a perfect stationary environment. Just that, if the environment were perfectly isolated, the wave function would still have a spread-out shape.” From Dick Lyon [personal communication]: “In the Gaussian case it may just be apparently random, not actually random, as long as there's a sum of many small contributions from other electrons in the universe.” Both of these comments are consistent with the Collective Electrodynamics framework of coherent wavefunctions and nonlocal interactions [Mead, 2000].
5. If it should turn out that none of the above proposals (or some mixture of the above proposals) is supported by the higher-order moments calculation, it would likely lead us to make a new proposal that would fit the new constraint.

The underlying physics of each of these proposals is dramatically different from the others. Which one (if any) is right? Quantum Electrodynamics appears to be silent on the question. We believe that answering this question would be very important.

10. Conclusions

We use perturbation analysis to show that the Lamb Shift is consistent with electron charge spreading inside the half-reduced Compton Wavelength, and we develop a novel numerical technique for solving the Dirac Hydrogen problem with a modified Coulomb potential, and use it to find the form of the modified Dirac Hydrogen wavefunctions. We show that the singularity at the origin of the Dirac Hydrogen wavefunction is eliminated, with a small amount of charge density near the origin displaced radially outward. The large component is made continuous at the origin, and the small component is driven to zero at the origin. The near-constant behavior of the Bethe Logarithm out to its asymptotic limit as principal quantum number $n \rightarrow \infty$ leads to a novel suggestion that this charge spreading for a bound electron in a Hydrogen Atom may also occur for a free electron. We also show novel 3D visualizations of numerical Dirac equation simulations.

References

1. Barut, A.O., and Bracken, A.J., "Zitterbewegung and the internal geometry of the electron", *Phys. Rev. D*, Vol. 23, No. 10, (1981), p. 2454-2463.
2. Bracken, A.J., Ellinas, D., and Smyrnakis, I., "Free Dirac Evolution as a Quantum Random Walk", arXiv:quant-ph/0605195v1, 2006.
3. Darwin, C. G., "The Wave Equations of the Electron", *Proc. Roy. Soc. A*118 (1928), p. 654-680.
4. Dirac, P.A.M., "The Quantum Theory of the Electron", *Proc. Roy. Soc. A*117 (1928), p. 610-624.
5. Eides, M., Grotch, H., and Shelyuto, V., *Theory of Light Hydrogenic Bound States*, Springer, 2007.
6. Ellinas, D., Bracken, A.J., and Smyrnakis, I., "Discrete Randomness in Discrete Time Quantum Walk: Study via Stochastic Averaging", arXiv:1207.5257v1, 2012.
7. Feynman, R., "Relativistic Cut-off for Quantum Electrodynamics", *Phys. Rev.* **74** (1948), p. 1430-1438.
8. Hammerling, R. et al., "Numerical Solution of Singular ODE Eigenvalue Problems in Electronic Structure Computations", *Computer Physics Communications* 181:1557-1561, 2010.
9. Hestenes, D., "Zitterbewegung in Quantum Mechanics", *Found. Phys.* (2010) 40:1.
10. Itzhikson and Zuber, "Quantum Field Theory", McGraw-Hill, 1980, p. 79.
11. Jentschura, U.D., and Mohr, P.J., "Bethe Logarithms for Rydberg States: Numerical Values for $n \leq 200$ ", arXiv:quant-ph/0504002v1 2005.
12. Lamb, W., and Retherford, R., "Fine Structure of the Hydrogen Atom by a Microwave Method". *Physical Review* **72** (1947): 241–243.
13. Landau and Lifshitz, "Course of Theoretical Physics", Vol. 4, 2nd Edition, 1982, p. 137.
14. Mead, C.A., *Collective Electrodynamics: Quantum Foundations of Electromagnetism*, MIT Press, 2000.
15. Patil, S.H., "Analytic Phase Shifts for Truncated and Screened Coulomb Potentials", *Phys. Rev. A* **24** (1981), p. 2913.
16. Silbar, R. R., and Goldman, T., "Solving the Radial Dirac Equations: A Numerical Odyssey", arXiv:1001.2514v2, 2010.
17. Thaller, B., "Advanced Visual Quantum Mechanics", Springer 2005.
18. Wannier, G.H., "Energy Eigenvalues for the Coulomb Potential with Cut-Off. Part I", *Phys. Rev.* **64** (1943), p. 358-366.
19. Welton, T.A., "Some Observable Effects of the Quantum-Mechanical Fluctuations of the Electromagnetic Field", *Phys. Rev.* **74**, p. 1157 – 1167.

Appendix – Perturbation Analysis for Gaussian Charge Density

$$rZ = \frac{\hbar}{2mc} * 0.218849 = 4.22553 \times 10^{-14} \text{m}$$

$$\mu r = \frac{a_0}{rZ} = 1253.02$$

$$V[r] = -\frac{\hbar \alpha \text{Erf}\left[\frac{r}{\sqrt{2} rZ}\right]}{r}$$

$$dV[r] = \frac{\hbar \alpha \left(1 - \text{Erf}\left[\frac{r}{\sqrt{2} rZ}\right]\right)}{r}$$

$$E1 = -\frac{1}{2} c^2 m r \alpha^2$$

$$\text{deltaE1} = -\frac{c^2 m r \alpha^2 \left(\left(2 \sqrt{\frac{2}{\pi}} - \mu r \right) \mu r + e^{\frac{2}{\mu r^2}} (-4 + \mu r^2) \text{Erfc}\left[\frac{\sqrt{2}}{\mu r}\right] \right)}{\mu r^2}$$

$$\mu r1Sval = 1267.24 \quad (\text{scaled } \mu r \text{ value for 1S state, accounts for lnk0 adjustment})$$

$$\Delta E1S = \frac{m c^2 (Z \alpha)^2}{h} \frac{1}{2 n^2} \left(-2 + \frac{4 \sqrt{\frac{2}{\pi}}}{\mu r} + 2 e^{\frac{2}{\mu r^2}} \text{Erfc}\left[\frac{\sqrt{2}}{\mu r}\right] - \frac{8 e^{\frac{2}{\mu r^2}} \text{Erfc}\left[\frac{\sqrt{2}}{\mu r}\right]}{\mu r^2} \right)$$

$$) = \frac{m c^2 (Z \alpha)^2}{h} \frac{4}{2 n^3 \mu r^2} = 8.17623 \text{ GHz (scaled)} \quad \text{target is } 8.17287 \text{ GHz}$$

$$\text{deltaE2} = -\frac{1}{8 \sqrt{\pi} \mu r^6}$$

$$c^2 m r \alpha^2 \left(\mu r (\sqrt{2} + 3 \sqrt{2} \mu r^2 + 2 \sqrt{2} \mu r^4 - 2 \sqrt{\pi} \mu r^5) + e^{\frac{1}{\mu r^2}} \sqrt{\pi} (-1 - 4 \mu r^2 - 3 \mu r^4 + 2 \mu r^6) \text{Erfc}\left[\frac{1}{\sqrt{2} \mu r}\right] \right)$$

$$\Delta E2S = \frac{m c^2 (Z \alpha)^2}{h} \frac{1}{2 n^2} \left(-2 + \frac{\sqrt{\frac{2}{\pi}}}{\mu r^5} + \frac{3 \sqrt{\frac{2}{\pi}}}{\mu r^3} + \frac{2 \sqrt{\frac{2}{\pi}}}{\mu r} + \right)$$

$$2 e^{\frac{1}{\mu r^2}} \text{Erfc}\left[\frac{1}{\sqrt{2} \mu r}\right] - \frac{e^{\frac{1}{\mu r^2}} \text{Erfc}\left[\frac{1}{\sqrt{2} \mu r}\right]}{\mu r^6} - \frac{4 e^{\frac{1}{\mu r^2}} \text{Erfc}\left[\frac{1}{\sqrt{2} \mu r}\right]}{\mu r^4} - \frac{3 e^{\frac{1}{\mu r^2}} \text{Erfc}\left[\frac{1}{\sqrt{2} \mu r}\right]}{\mu r^2}$$

$$) = \frac{m c^2 (Z \alpha)^2}{h} \frac{4}{2 n^3 \mu r^2} = 1.04534 \text{ GHz} \quad \text{target is } 1.04503 \text{ GHz}$$

$$\Delta E = \frac{m c^2 (Z \alpha)^2}{h} \frac{4}{2 n^3 \mu r^2} \quad \epsilon_{\text{general}} = -\frac{4}{\mu r^2}$$

$$\text{Distribution Factor Df} = \frac{4}{Z^2} \quad \text{target Df} = 26 \alpha = 0.189731$$

